

# Effects of *HMGA2* gene silencing on cell cycle and apoptosis in the metastatic renal carcinoma cell line ACHN

Journal of International Medical Research

50(2) 1–14

© The Author(s) 2022

Article reuse guidelines:

[sagepub.com/journals-permissions](https://sagepub.com/journals-permissions)

DOI: 10.1177/03000605221075511

[journals.sagepub.com/home/imr](https://journals.sagepub.com/home/imr)



Qian Chen\*, Qizhong Fu\*, Lin Pu,  
Xianfeng Liu and Ying Liu 

## Abstract

**Objective:** To explore the role of high mobility group AT-hook 2 (*HMGA2*) in the regulation of the cell cycle and apoptosis.

**Methods:** The renal carcinoma cell line ACHN was transiently transfected with small interfering RNA to knock down the expression of the *HMGA2* gene. Cell cycle analysis was undertaken using flow cytometry. The mRNA and protein levels of *HMGA2*, E2F transcription factor 1 (*E2F1*), cyclin D1, cyclin dependent kinase 6 (*CDK6*), B-cell lymphoma-2 (*Bcl-2*), caspase-3 and caspase-9 were analysed using reverse transcription quantitative real-time polymerase chain reaction and Western blot analysis.

**Results:** The mRNA and protein levels of *HMGA2* were significantly higher in renal carcinoma cell lines compared with the human renal proximal tubular epithelial cell line HKC. After *HMGA2* gene-specific silencing, more cells entered the G<sub>0</sub>/G<sub>1</sub> phase, while fewer cells entered the G<sub>2</sub>/M phase; and the cells exhibited early and late apoptosis. *HMGA2* gene-specific silencing significantly reduced the mRNA and protein levels of *E2F1*, cyclin D1, *CDK6* and *Bcl-2*; and increased the mRNA and protein levels of caspase-3 and caspase-9.

**Conclusion:** The *HMGA2* gene may be involved in the tumorigenesis and development of renal cancer, thus inhibiting *HMGA2* gene expression might provide a potential therapeutic target in the future.

\*These authors contributed equally to this work.

## Corresponding author:

Ying Liu, Department of Urology Surgery, The Affiliated Zhongshan Hospital of Dalian University, 6 Jiefang Street, Zhongshan District, Dalian, Liaoning 116001, China.  
Email: 13962031491@163.com

Department of Urology Surgery, The Affiliated Zhongshan Hospital of Dalian University, Dalian, Liaoning Province, China



Creative Commons Non Commercial CC BY-NC: This article is distributed under the terms of the Creative Commons Attribution-NonCommercial 4.0 License (<https://creativecommons.org/licenses/by-nc/4.0/>) which permits non-commercial use, reproduction and distribution of the work without further permission provided the original work is attributed as specified on the SAGE and Open Access pages (<https://us.sagepub.com/en-us/nam/open-access-at-sage>).

## Keywords

Renal carcinoma, HMGA2, RNAi, cell cycle arrest, apoptosis

Date received: 25 September 2021; accepted: 6 January 2022

## Introduction

High mobility group AT-hook 2 (HMGA2) is a non-histone protein that binds to chromosomes, but lacks transcriptional activity itself.<sup>1</sup> HMGA2 can regulate the transcription of target genes by binding to DNA and can change the structure of chromatin to bend, stretch, curl, loop or unchain.<sup>2</sup> Hence, it is also called the constructive transcription factor.<sup>3</sup> HMGA2 plays an important role in tumorigenesis, the cell cycle and apoptosis, and has become one of the most studied oncogenes in recent years.<sup>4</sup> Previous studies have reported that HMGA2 was upregulated in renal carcinoma compared with either being at low levels or absent in benign renal neoplasms and healthy renal tissues, making HMGA2 a biomarker for renal carcinoma.<sup>5-9</sup>

Due to the occult onset of renal cell carcinoma, there are no special symptoms in the early stage. The main reason for this is that the biological behaviour of renal carcinoma is highly changeable and the traditional histopathological stages and grades have some limitations in predicting the biological behaviour of renal carcinoma.<sup>10,11</sup> At present, surgical therapy is the main treatment for renal carcinoma. During a median follow-up of 62 months, 25.3% and 41.5% patients with clinical stage T1a renal cancer died following partial or radical nephrectomy, respectively.<sup>12</sup> Moreover, since renal carcinoma cells are insensitive to radiotherapy and chemotherapy,<sup>13</sup> in-depth studies examining the molecular mechanism underlying the development of renal carcinoma could provide novel gene targets and

therapeutic choices for clinical treatment in renal carcinoma.

This current study investigated the role of HMGA2 in cell cycle regulation and apoptosis in the human metastatic renal carcinoma cell line ACHN using *HMGA2* gene silencing with RNA interference (RNAi) methodology. E2F transcription factor 1 (E2F1), cyclin D1, cyclin dependent kinase 6 (CDK6), B-cell lymphoma-2 (Bcl-2), caspase-3 and caspase-9 mRNA and protein levels were measured in order to determine their roles in the regulation of the cell cycle and apoptosis.

## Materials and methods

### Cell lines and culture conditions

The human renal proximal tubular epithelial cell line (HKC), human renal carcinoma cell lines (786-O and 769-P) and the ACHN cell line were purchased from Chenyu Biotechnology (Dalian, China) and Jiangsu Kaiji Biotechnology (Nanjing, China). The HKC, 786-O, 769-P and ACHN cell lines were cultured in RPMI-1640 (Jiangsu Kaiji Biotechnology) medium supplemented with 10% fetal calf serum (Jiangsu Kaiji Biotechnology) at 37°C with 5% CO<sub>2</sub>. The adherent cells were sub-cultured once every 2–3 days.

### Transient transfection with small interfering RNA (siRNA)

Cells were assigned to three groups: HMGA2-siRNA group, mock-siRNA group and non-transfected control group

(HMGA2-siRNA and mock-siRNA; Jima Pharmaceutical Technology, Shanghai, China). RNAi was applied for transient transfection in ACHN cells. Transient cell transfection was implemented according to the instructions of the Lipofectamine<sup>®</sup> 2000 reagent kit (Thermo Fisher Scientific, Rockford, IL, USA). Briefly, two high-pressure sterilized Eppendorf tubes were used; and 10  $\mu$ l siRNA + 240  $\mu$ l serum-free RPMI-1640 medium and 10  $\mu$ l Lipofectamine<sup>®</sup> + 240  $\mu$ l serum-free RPMI-1640 were added to each tube, respectively. After gentle mixing, these tubes were incubated at room temperature for 20 min to form an siRNA-Lipofectamine<sup>®</sup> complex. The mixed liposomes and siRNA solution were added to each well dropwise and cultured in an incubator. Then, the RNA was extracted after 24 h for subsequent reverse transcription quantitative real-time polymerase chain reaction (RT-qPCR) (Thermo Fisher Scientific) analysis as described below. The protein was extracted after 48 h for Western blot analysis as described below.

### *RNA extraction and RT-qPCR analysis of mRNA levels*

Total RNA was extracted from  $1.0 \times 10^7$  cells using TRIzol<sup>™</sup> reagent (Thermo Fisher Scientific). The concentration of the RNA sample was measured using a spectrophotometer. Then, 5  $\mu$ l RNA samples were collected and added into 495  $\mu$ l 1X TE buffer. Next, 2  $\mu$ g RNA was reverse transcribed into cDNA. The specific procedures were performed as described by instructions of the corresponding kit (RT kit/PCR kit/The quantitative real-time PCR kit; Takara Bio, Dalian, China). The HMGA2 sequence number is NM001300918.1 and the length of the primer (Aoke Biotechnology, Beijing, China) was 85 base pairs (bp). The forward primer sequence for HMGA2 was

5'-TCCACTTCAGCCCAGGGACAAC-3'; and the reverse primer sequence was 5'-TGGTTCTTGCTGCTGCTTCCT-3'. The glyceraldehyde 3-phosphate dehydrogenase (GAPDH) sequence number is NM001101.4 and the length of the primer was 90 bp. The forward primer sequence for GAPDH was 5'-AGATCATCAGCAATGCCTCCT-3'; and the reverse primer sequence was 5'-TGAGTCCTTCCACGATACCAA-3'. The length of the primer of the E2F1 was 111 bp. The forward primer sequence for E2F1 was 5'-CCTGAGGGATCAAAGCCTGGAA-3'; and the reverse primer sequence was 5'-TGGAGCCTGAGACACGATTCTG-3'. The length of the primer of the cyclin D1 was 96 bp. The forward primer sequence for cyclin D1 was 5'-CCATTCACGCCGCCAGTTGT-3'; and the reverse primer sequence was 5'-TTCC TGCCATTCTGCTCTCCT-3'. The length of the primer of the CDK6 was 98 bp. The forward primer sequence for CDK6 was 5'-ACGACCTAACCTGCTGCCTGT-3'; and the reverse primer sequence was 5'-AGTTCCCACCTGCCACTGTT-3'. The length of the primer of the Bcl-2 was 82 bp. The forward primer sequence for Bcl-2 was 5'-TGGACAACATCGCCCTGTGGAT-3'; and the reverse primer sequence was 5'-GCATCCCAGCCTCCGTTATCCT-3'. The length of the primer of caspase-3 was 120 bp. The forward primer sequence for caspase-3 was 5'-GCCGTGGTACAGAATGGACTG-3'; and the reverse primer sequence was 5'-AACCAGGTGCTGTGGAGTATGC-3'. The length of the primer of caspase-9 was 120 bp. The forward primer sequence for caspase-9 was 5'-TTGGTGTGTCGGTGCTCTTGA-3'; and the reverse primer sequence was 5'-CGGACTCACGGCAGAAGTTCA-3'. The cycling programme (ABI Veriti 96 well thermal cycler; Thermo Fisher Scientific) involved preliminary denaturation at 95°C for 5 min, followed by 40 cycles of denaturation at 95°C for 15 s, annealing at 60°C for 20 s, and

elongation at 72°C for 40s, followed by a final elongation step at 60°C for 1 min. Each sample was repeated three times. The PCR products were visualized under UV light (SHIMADZU, Shanghai, China). A fluorescence quantitative PCR thermal cycler (ABI Step one plus real time-PCR system; Thermo Fisher Scientific) was used to quantify the PCR products. The product specificity was analysed using the dissolution curve and the Cq value was recorded when the reaction was finished. The comparative  $\Delta\Delta Cq$  method was applied for relative quantitative analysis and the  $2^{-\Delta\Delta Cq}$  method was used to compute the relative mRNA levels in each sample. GAPDH was used as the internal reference. During the PCR analysis, the corresponding internal reference was used for each sample, each time.  $\Delta\Delta Cq = (Cq \text{ of the experimental HMGA2 gene} - Cq \text{ of the experimental internal reference}) - (Cq \text{ of the control HMGA2 gene} - Cq \text{ of the control internal reference})$ .

### **Western blot analysis of cellular protein levels**

At 48 h after the transfection of HMGA2-siRNA and mock-siRNA, the ACHN cells were collected. Then, the cells were lysed using RIPA lysis buffer (Jiangsu Kaiji Biotechnology). The total protein was extracted from  $1.0 \times 10^7$  cells in each well and quantified using the BCA method (Jiangsu Kaiji Biotechnology). Protein samples were separated by sodium dodecyl sulphate-polyacrylamide gel electrophoresis. The proteins were transferred to polyvinylidene fluoride membranes using a Trans-blot Turbo universal protein transfer system (Bio-Rad, Hercules, CA, USA) at 200 mA constant flow for 2 h. Blocking was performed for 1 h at 25°C with Tris-buffered saline/0.1% Tween-20 (pH 7.5; TBST) containing 5% skimmed milk powder (Jiangsu Kaiji Biotechnology).

The membrane was then incubated with rabbit anti-human HMGA2 primary antibody (1:1000 dilution; Thermo Fisher Scientific) at 4°C overnight. The membrane was washed three times with TBST for 10 min at 25°C. The membrane was then incubated with goat anti-rabbit secondary antibody (1:3000 dilution; Thermo Fisher Scientific) at room temperature for 1 h. After washing three times with TBST for 5 min at 25°C, the ECL Chemiluminescence Kit (Thermo Fisher Scientific) and G:BOX chemiXR5 imaging system (Syngene, Cambridge, UK) was used for image analysis and the Gel-Pro32 software version 6.0 (Media Cybernetics, Houston, TX, USA) was used for the grayscale analysis. A rabbit anti-human GAPDH monoclonal antibody (1:1000 dilution; Novo Biotechnology, Beijing, China) was used as the internal reference followed by goat anti-rabbit secondary antibody (1:3000 dilution; Thermo Fisher Scientific). Following the same experimental steps as described above, rabbit anti-E2F1 (1:2000 dilution; Abcam, Cambridge, UK), rabbit anti-cyclin D1 (1:1000 dilution; Abcam), rabbit anti-CDK6 (1:1000 dilution; Abcam), rabbit anti-Bcl-2 (1:2000 dilution; Abcam), rabbit anti-cleaved-caspase-9 (1:500 dilution; Abcam) and rabbit anti-cleaved-caspase-9 (1:2000 dilution; Abcam) were used as primary antibodies followed by goat anti-rabbit IgG-horseradish peroxidase (1:5000 dilution; Jiangsu Kaiji Biotechnology) secondary antibody. Rabbit anti-human GAPDH (1:5000 dilution; Jiangsu Kaiji Biotechnology) was used as internal reference. Experiments were performed in triplicate to detect the protein levels.

### **Cell cycle detection using PI staining**

After 48 h of transfection in 6-well plates, cells were digested with ethylenediaminetetra-acetic acid (EDTA)-free trypsinase for 2 min and

collected via centrifugation for 5 min at 4°C at 550 *g* (Sorvall™ ST 16 Centrifuge; Thermo Fisher Scientific). Cells were washed three times with 0.01 mM phosphate-buffered saline (PBS; pH 7.2) for 10 s at 4°C. Then, pre-cooled 70% ethanol was added and the cells were dispersed rapidly into a single cell suspension, followed by fixation at -20°C overnight. After centrifugation for 10 min at 550 *g* (Sorvall™ ST 16 Centrifuge; Thermo Fisher Scientific), the fixative solution was discarded and any residual ethanol was thoroughly removed by washing the cell pellet three times with 0.01 mM PBS (pH 7.2) for 10 s at 4°C. Then, 600 µl of 0.075 mM propidium iodide (PI; Beijing Baiaolaibo Technology, Beijing, China) was added to the cells and they were placed in the dark at 4°C for 1 h. Flow cytometry was used to detect the red fluorescence and light scattering at an excitation wavelength of 488 nm using a BD FACSCalibur™ Flow Cytometer (Becton, Dickinson and Company, Franklin Lakes, NJ, USA). Subsequently, the percentages of cells in the G<sub>0</sub>/G<sub>1</sub> phase, S phase and G<sub>2</sub>/M phase in the HMGA2-siRNA group, mock-siRNA group and non-transfected control group were calculated.

### *Cell apoptosis detection using annexin V-FITC*

After 48 h of transfection in 6-wells plates, cells were digested with EDTA-free trypsinase for 2 min and collected via centrifugation at 977 *g* for 5 min at 4°C (Sorvall™ ST 16 Centrifuge; Thermo Fisher Scientific). Then, cells were washed twice with 0.01 mM PBS (pH 7.2) for 10 s at 4°C and then centrifuged again at 977 *g* for 5 min at 4°C. Subsequently, the supernatant was removed and the cell pellet was retained. Then, 100 µl 1X binding buffer was added to resuspend the cells, followed by 5 µl annexin V/7-AAD (Annexin V-FITC/7-AAD

Apoptosis Detection Kit; Sino Biological, Beijing, China) and 5 µl 0.075 mM PI solution. These solutions were gently mixed with the cells and then allowed to react at room temperature in the dark for 10 min. Next, 400 µl 1X binding buffer was added and evenly mixed before flow cytometry detection at an excitation wavelength of 488 nm using a BD FACSCalibur™ Flow Cytometer (Becton, Dickinson and Company). The green fluorescence of the fluorescein isothiocyanate (FITC) was detected in the FL1 channel, while the red fluorescence of the 7-AAD was detected in the FL3 channel. Cells that were annexin V-positive and 7-AAD-negative were regarded as apoptotic cells in the early phase, while annexin V and 7-AAD double positive cells were regarded as apoptotic cells in the later phase. The apoptotic rate was the sum of these two parts.

### *Statistical analyses*

All statistical analyses were performed using the SPSS® statistical package, version 17.0 (SPSS Inc., Chicago, IL, USA) for Windows®. Continuous data are presented as mean ± SD and evaluated using the Shapiro-Wilk test in order to confirm a normal distribution. Student's *t*-test was used to compare two independent groups. Multiple group mean comparisons were performed using one- or two-way analysis of variance. The least significant difference method was used for multiple comparisons. A *P*-value <0.05 was considered statistically significant.

### **Results**

To obtain the baseline HMGA2 mRNA levels in the studied cell lines, Cq values were retrieved using the RT-qPCR amplification curve. The mean ± SD relative mRNA levels of HMGA2 in ACHN cells, 786-O cells, 769-P cells and HKC cells were

$1.00 \pm 0.06$ ,  $0.90 \pm 0.03$ ,  $0.79 \pm 0.05$  and  $0.06 \pm 0.01$ , respectively (Figure 1a). The HMGA2 mRNA levels in the renal carcinoma cell lines were significantly higher compared with that in the normal renal tubular epithelial cell line HKC ( $P < 0.01$  for all comparisons).

Western blot analysis was undertaken to determine if there was a similarity between HMGA2 mRNA and protein levels in the studied cell lines. The mean  $\pm$  SD relative protein levels of HMGA2 in ACHN cells, 786-O cells, 769-P cells and HKC cells were  $0.72 \pm 0.07$ ,  $0.65 \pm 0.05$ ,  $0.57 \pm 0.04$  and  $0.04 \pm 0.01$ , respectively (Figure 1b).

In accordance with the RT-qPCR results, the HMGA2 protein levels in the renal carcinoma cell lines were significantly higher compared with that in the normal renal tubular epithelial cell line HKC ( $P < 0.01$  for all comparisons).

Based on the results that showed that both the HMGA2 mRNA and protein levels were higher in ACHN cells compared with 786-O and 769-P cells, ACHN cells were selected for further siRNA interference studies. In total, three gene segments of HMGA2, HMGA2-siRNA1, HMGA2-siRNA2 and HMGA2-siRNA3, as well as mock-siRNA were selected.

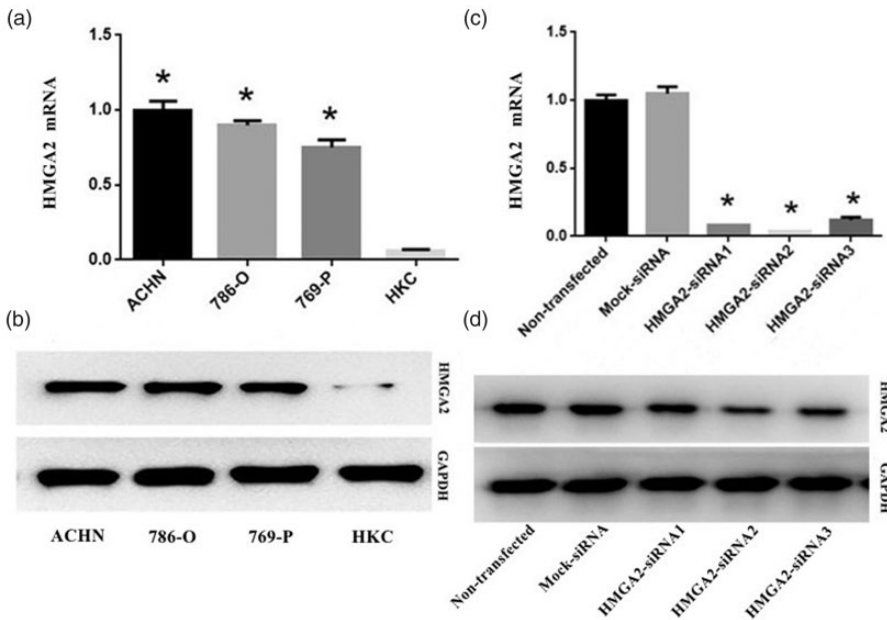


**Figure 1.** The levels of high mobility group AT-hook 2 (HMGA2) mRNA and protein before and after small interfering RNA (siRNA) interference in ACHN, 786-O, 769-P and HKC cell lines: (a) reverse transcription quantitative real-time polymerase chain reaction (RT-qPCR) analysis of the mRNA levels of HMGA2 before siRNA interference. Data presented as mean  $\pm$  SD. \* $P < 0.01$  compared with HKC group, Student's *t*-test; (b) Western blot analysis of protein levels of HMGA2 before siRNA interference. GAPDH, glyceraldehyde 3-phosphate dehydrogenase; (c) RT-qPCR analysis of the mRNA levels of HMGA2 after siRNA interference in the mock-siRNA, HMGA2-siRNA1, HMGA2-siRNA2 HMGA2-siRNA3 or non-transfected groups of ACHN cells. Data presented as mean  $\pm$  SD. \* $P < 0.01$  compared with the non-transfected and mock-siRNA groups, Student's *t*-test; (d) Western blot analysis of protein levels of HMGA2 after siRNA interference in the mock-siRNA, HMGA2-siRNA1, HMGA2-siRNA2 HMGA2-siRNA3 or non-transfected groups of ACHN cells.

The sequence information is presented in Table 1.

Total RNA was extracted from ACHN cells 24 h after transfection with HMGA2-siRNA and mock-siRNA. The mean  $\pm$  SD relative HMGA2 mRNA levels as determined using RT-qPCR in the non-transfected control group, mock-siRNA group, HMGA2-siRNA1 group, HMGA2-siRNA2 group and HMGA2-siRNA3 group, were  $1.00 \pm 0.04$ ,  $1.05 \pm 0.05$ ,  $0.08 \pm 0.00$ ,  $0.04 \pm 0.00$  and  $0.12 \pm 0.02$ , respectively (Figure 1c). The HMGA2 mRNA levels in the transfected HMGA2-siRNA groups were significantly lower compared with those in the transfected mock-siRNA group and the non-transfected control group ( $P < 0.01$  for all comparisons).

Total protein was extracted from cells 48 h after transfection with HMGA2-siRNA and mock-siRNA for Western blot analysis. The mean  $\pm$  SD relative HMGA2 protein levels in the non-transfected control group, mock-siRNA group, HMGA2-siRNA1 group, HMGA2-siRNA2 group and HMGA2-siRNA3 group were  $0.75 \pm 0.09$ ,  $0.68 \pm 0.07$ ,  $0.07 \pm 0.02$ ,  $0.02 \pm 0.00$  and  $0.11 \pm 0.04$ , respectively (Figure 1d). The HMGA2 protein levels in the transfected HMGA2-siRNA groups were significantly lower compared with those in the transfected mock-siRNA group and non-transfected control group ( $P < 0.01$  for all comparisons). These results suggested that HMGA2 mRNA and protein levels were successfully knocked down by the siRNA interference. Compared with the other two

HMGA2-siRNA groups, the mRNA and protein levels were the lowest in the HMGA2-siRNA2 transfection group so this gene segment was selected for subsequent studies.

To study the effects of HMGA2 on the cell cycle, the ACHN cells in each group were collected after 48 h of transfection and changes in the cell cycle were detected using flow cytometry after PI staining. As presented in Figures 2a–2c and 3A, compared with those in the mock-siRNA group and non-transfected group, the HMGA2-siRNA group had a significantly increased number of cells in the  $G_0/G_1$  phase and a decreased number of cells in the  $G_2/M$  phase ( $P < 0.05$  for all comparisons), suggesting that HMGA2-siRNA led the arrest of ACHN cells in the  $G_1$  phase. These data were obtained from  $\geq 3$  independent experiments.

To investigate whether HMGA2 affects the apoptosis of ACHN cells, HMGA2 was knocked down in ACHN cells and apoptosis was analysed using annexin V-FITC. As shown in Figures 2d–2f, the upper left quadrant represented a group of mechanically damaged cells, the upper right quadrant represented a group of necrotic cells, the lower left quadrant represented a group of living cells and the lower right quadrant represented a group of apoptotic cells. The total apoptotic rate in HMGA2-knockdown ACHN cells increased from 5.69% in the non-transfected group to 16.52% in the HMGA2-siRNA group ( $P < 0.05$ ).

**Table 1.** Sequence information for the small interfering RNA (siRNA) used in this study.

siRNA	Sense (5'–3')	Antisense (3'–5')
HMGA2-siRNA1	CCU AAG AGA CCC AGG GGA ATT	UUC CCC UGG GUC UCU UAG GTT
HMGA2-siRNA2	GCA GAA GCC ACU GGA GAA ATT	UUU CUC CAG UGG CUU CUG CTT
HMGA2-siRNA3	CCA GGA AGC AGC AGC AAG ATT	UCU UGC UGC UGC UUC CUG GTT
Mock-siRNA	GAAGGTGAAGGTCGGAGTC	GAAGATGGTGTATGGGATTC

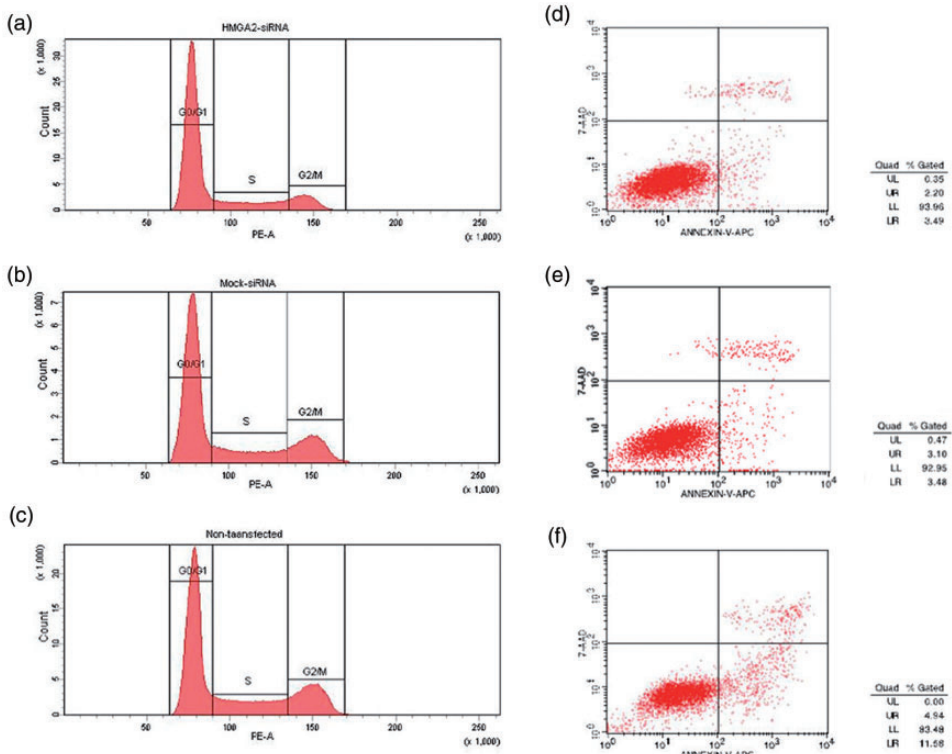


**Figure 2.** Flow cytometric analysis of the effects of high mobility group AT-hook 2 (HMGA2) knock down on cell cycle and apoptosis in ACHN cells. The cell cycle was analysed using propidium iodide staining: (a) ACHN cells transfected with HMGA2-small interfering RNA (siRNA); (b) ACHN cells transfected with mock-siRNA; (c) non-transfected ACHN cells. Apoptosis was detected using annexin V/7-AAD staining: (d) non-transfected ACHN cells; (e) ACHN cells transfected with mock-siRNA; (f) ACHN cells transfected with HMGA2-siRNA.

To elucidate the molecular mechanism involved in the effect of HMGA2 on the cell cycle, the effects of HMGA2 knock-down on the mRNA levels of cell cycle regulators, including E2F1, cyclin D1 and CDK6, were studied. HMGA2 knockdown significantly reduced the mRNA levels of E2F1, cyclin D1 and CDK6 in ACHN cells ( $P < 0.05$  for all comparisons) (Figure 3b). The protein levels of E2F1, cyclin D1 and CDK6 in ACHN cells were significantly attenuated compared with non-transfected control and mock-siRNA groups ( $P < 0.05$  for all comparisons) (Figure 3c).

To elucidate the molecular mechanism involved in the effect of HMGA2 on apoptosis, the effects of HMGA2 knockdown on the levels of apoptosis regulators, including Bcl-2, caspase-3 and caspase-9, were studied. HMGA2-siRNA results in lower levels of Bcl-2 mRNA but higher levels of caspase-3 and caspase-9 mRNA in ACHN cells ( $P < 0.05$  for all comparisons) (Figure 3d). HMGA2-siRNA results in lower levels of Bcl-2 protein but higher levels of caspase-3 and caspase-9 protein in ACHN cells ( $P < 0.05$  for all comparisons) (Figure 3e).

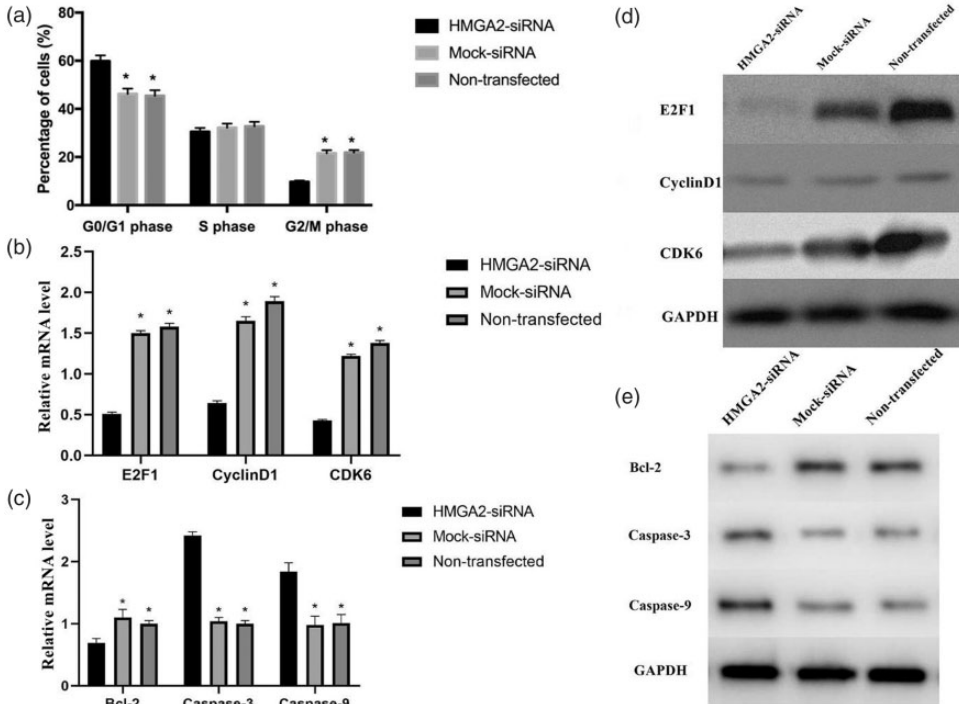


**Figure 3.** The effects of high mobility group AT-hook 2 (HMGA2) knock down on cell cycle and apoptosis regulatory factors in ACHN cells. (a) Proportion of ACHN cells in the three cell cycle phases after small interfering RNA (siRNA) interference in the mock-siRNA, HMGA2-siRNA or non-transfected groups. Data presented as mean  $\pm$  SD. \* $P < 0.05$  compared with HMGA2-siRNA group, Student's *t*-test. (b) Reverse transcription quantitative real-time polymerase chain reaction (RT-qPCR) analysis of cell cycle regulation-related mRNA levels (E2F transcription factor 1 [E2F1], cyclin D1, cyclin dependent kinase 6 [CDK6]) after siRNA interference in ACHN cells. Data presented as mean  $\pm$  SD. \* $P < 0.05$  compared with HMGA2-siRNA group, Student's *t*-test. (c) RT-qPCR analysis of apoptosis regulation-related mRNA levels (B-cell lymphoma-2 [Bcl-2], caspase-3, caspase-9) after siRNA interference in ACHN cells. Data presented as mean  $\pm$  SD. \* $P < 0.05$  compared with HMGA2-siRNA group, Student's *t*-test. (d) Western blot analysis of cell cycle regulation-related protein levels (E2F1, cyclin D1, CDK6) after siRNA interference in ACHN cells. GAPDH, glyceraldehyde 3-phosphate dehydrogenase. (e) Western blot analysis of apoptosis regulation-related protein levels (Bcl-2, caspase-3, caspase-9) after siRNA interference in ACHN cells.

## Discussion

Renal carcinoma is one of the most common malignant neoplasms of the urogenital system.<sup>14</sup> Several recent studies have reported that HMGA2 is highly expressed in renal carcinoma.<sup>15–17</sup> However, the underlying molecular mechanisms remain to be elucidated. As a structural transcription factor, HMGA2 can regulate the transcription and activation of a large number

of genes, especially those associated with cell cycle and apoptosis.<sup>18,19</sup>

Cyclin D1 and CDK6 are key proteins that regulate the progression of the cell cycle and they interact to form the cyclin D1-CDK6 complex, which affects the transformation of cells from G1 phase to S phase.<sup>20,21</sup> Transcription factor E2F1 is an important factor involved in cell cycle regulation.<sup>22</sup> E2F1 is able to enhance the levels

of key cell cycle regulators, such as cyclin D, cyclin A and CDK, which makes it of great significance for cell cycle, proliferation and apoptosis regulation.<sup>23,24</sup> Cell cycle disturbance is considered to be a common feature of tumorigenesis and accumulating evidence suggests that HMGA2 promotes tumour cell proliferation by up-regulating the levels of cell cycle-related genes.<sup>25</sup> The detailed mechanisms are as follows: (i) HMGA2 may activate the transcription factor E2F1 to promote cell dysplasia, thereby inducing the transformation of the cell cycle G2/M phase and inducing tumour growth;<sup>26</sup> (ii) HMGA2 increases the levels of cyclin D1 and CDK6, promotes the formation of the cyclin D1-CDK6 complex, accelerates the process of cell cycle G1, promotes the transformation of G2/M phase, interferes with cell cycle and promotes tumorigenesis;<sup>27</sup> (iii) the overexpression of HMGA2 may destroy the DNA repair system.<sup>28</sup>

Previous studies reported that the level of HMGA2 in renal carcinoma was higher compared with that in benign renal neoplasms and normal renal tissues; and the level of HMGA2 was correlated with TNM stage and lymph node metastasis.<sup>29,30</sup> For example, the higher the tumour stage, the higher the level of HMGA2 and the shorter the survival time of patients.<sup>5</sup> Therefore, it was suggested that HMGA2 may contribute to the development of renal carcinoma. More interestingly, HMGA2 knockdown caused the arrest of ACHN cells in the G<sub>1</sub> phase in the current study. Thus, it was suggested that HMGA2 may play an oncogenic role in the development of renal carcinoma. The dysregulation of the cell cycle and the inhibition of apoptosis are the key factors that make the treatment of renal carcinoma difficult.<sup>14,31,32</sup> Therefore, the present study aimed to further investigate the effect of the *HMGA2* gene on the biological characteristics of renal carcinoma, so as to clarify

the molecular mechanism of its oncogenic effect.

To further elucidate the molecular mechanisms of HMGA2 in the pathogenesis of renal carcinoma, experiments in the current study were undertaken to detect the dynamic levels of three key cell cycle-related proteins in the HMGA2-knockdown ACHN cells. The present results demonstrated that HMGA2 knockdown significantly reduced the mRNA levels of E2F1, cyclin D1 and CDK6 in ACHN cells ( $P < 0.05$ ), suggesting that HMGA2 may promote the occurrence and development of renal carcinoma via the E2F1/cyclin D1/CDK6 signalling pathway, and this may be a potential therapeutic target for renal carcinomas.

Apoptosis is an active suicide form of cell death for physiological cells and is regulated primarily by cell cycle regulators.<sup>33</sup> The dynamic balance between cell proliferation and apoptosis is important for normal development, homeostasis maintenance, the formation of immune tolerance and the onset of malignant tumours in organisms.<sup>34</sup> Dysregulation of apoptosis is critical in tumorigenesis and development, and DNA breakage is a key feature of apoptosis in the late stage.<sup>35</sup> The *HMGA2* gene is widely expressed during embryonic development, while its expression is low or absent in mature tissues.<sup>36,37</sup> Previous studies have shown that HMGA2 may inhibit cell apoptosis mainly by destroying the DNA repair system.<sup>38,39</sup> In the present study, annexin V/7-AAD and PI staining was used to analyse the three groups of ACHN cells via flow cytometry. It was found that the apoptotic rate in the HMGA2-siRNA group was significantly higher compared with that in the mock-siRNA and non-transfected control groups, suggesting that a high expression level of the *HMGA2* gene could inhibit the apoptosis of renal carcinoma cells.

B-cell lymphoma-2 is one of the most important oncogenes in the study of

apoptosis and the main target molecule in the study of the molecular mechanisms of apoptosis.<sup>40,41</sup> The caspase family of proteins is a group of proteases with similar structures that exist in the cytoplasm and are involved in the regulation of cell growth, differentiation and apoptosis.<sup>42,43</sup> Among them, caspase-3 and caspase-9 are the key enzymes involved in apoptosis.<sup>44-46</sup> Once the signal transduction pathway is activated, caspase-3 and caspase-9 are activated.<sup>44-46</sup> This is followed by a cascade of apoptotic proteases, in which enzymes are activated to degrade important proteins in the cell and eventually lead to irreversible apoptosis.<sup>41,42,44</sup> HMGA2 can affect apoptosis through the Bcl-2-caspase-3-caspase-9 signalling pathway and promote the occurrence and development of renal cancer cells.<sup>18,30,41,43,47</sup> The findings of the current study showed that low levels of HMGA2 mRNA and protein reduced the levels of Bcl-2 mRNA and protein in HMGA2-siRNA transfected ACHN cells, which activated the downstream genes for caspase-3 and caspase-9, initiating the caspase cascade reaction. The inverse correlation between the mRNA and protein levels of Bcl-2 and the two caspases demonstrated in the current study appears to promote the apoptosis of renal cancer cells. These current findings suggest that HMGA2 may promote the occurrence and development of renal carcinoma via the Bcl-2-caspase-3-caspase-9 signalling pathway and this may be a potential therapeutic target for renal carcinomas.

Currently, there are many ways to treat cancer, including surgery, radiotherapy, chemotherapy, targeted therapy and immunotherapy. Compared with other treatment methods, targeted therapy has the advantages of providing more specific treatment effects and reduced side-effects.<sup>48</sup> Therefore, it is important that the therapeutic targets of renal cancer are studied in detail. At present, a variety of potential

therapeutic targets for renal cancer, including SMAD Family Member 2 (*SMAD2*), *SMAD3*, *Snail*, transforming growth factor receptor, E-cadherin and N-cadherin, are being actively investigated.<sup>49-51</sup> According to the reports published to date, the molecular mechanisms involved in the development of renal cancer are very complex and may even contain multiple signalling pathways.<sup>52-54</sup> Elucidating the mechanisms involved will involve the joint research efforts of multiple laboratories around the world.

This current study had several limitations. First, the effects of HMGA2 on cell cycle and apoptosis regulation in renal cancer were only explored in detail in the ACHN cell line. Additional cell lines, such as 786-O and 769-P, were not included to verify the results, so this will need to be addressed in future work. Secondly, only *in vitro* experiments were undertaken, so *in vivo* experiments will be the focus of future research.

In conclusion, the levels of HMGA2 mRNA and protein in human renal carcinoma cell lines were significantly higher compared with those in a normal human renal tubular epithelial cell line. HMGA2-siRNA interference knocked down *HMGA2* gene expression in ACHN cells, which disturbed the cell cycle and induced cell apoptosis. These current findings suggest that the *HMGA2* gene may be involved in the tumorigenesis and development of renal cancer, thus inhibiting *HMGA2* gene expression might provide a potential therapeutic target in the future.

#### **Declaration of conflicting interest**

The authors declare that there are no conflicts of interest.

#### **Funding**

The authors disclosed receipt of the following financial support for the research, authorship, and/or publication of this article: This research

was funded by the Dalian Science and Technology Bureau, China (grant no. 09-1110).

## ORCID iD

Ying Liu  <https://orcid.org/0000-0002-7874-9199>

## References

- Grosschedl R, Giese K and Pagel J. HMG domain proteins: architectural elements in the assembly of nucleoprotein structures. *Trends Genet* 1994; 10: 94–100. DOI: 10.1016/0168-9525(94)90232-1. PMID: 8178371.
- Unachukwu U, Chada K and D'Armiento J. High Mobility Group AT-Hook 2 (HMGA2) Oncogenicity in Mesenchymal and Epithelial Neoplasia. *Int J Mol Sci* 2020; 21: 3151. DOI: 10.3390/ijms21093151.
- Fedele M, Paciello O, De Biase D, et al. HMGA2 cooperates with either p27<sup>kip1</sup> deficiency or Cdk4<sup>R24C</sup> mutation in pituitary tumorigenesis. *Cell Cycle* 2018; 17: 580–588. DOI: 10.1080/15384101.2017.1403682.
- Mansoori B, Mohammadi A, Ditzel HJ, et al. HMGA2 as a Critical Regulator in Cancer Development. *Genes (Basel)* 2021; 12: 269. DOI: 10.3390/genes12020269.
- Liu Y, Fu QZ, Pu L, et al. HMGA2 Expression in Renal Carcinoma and its Clinical Significance. *J Med Biochem* 2015; 34: 338–343. DOI: 10.2478/jomb-2014-0036.
- Zhao H, Zhao H, Xia X, et al. MicroRNA-599 targets high-mobility group AT-hook 2 to inhibit cell proliferation and invasion in clear cell renal carcinoma. *Mol Med Rep* 2018; 17: 7451–7459. DOI: 10.3892/mmr.2018.8755.
- Massari F, Rizzo A, Mollica V, et al. Immune-based combinations for the treatment of metastatic renal cell carcinoma: a meta-analysis of randomised clinical trials. *Eur J Cancer* 2021; 154: 120–127. DOI: 10.1016/j.ejca.2021.06.015.
- Massari F, Mollica V, Rizzo A, et al. Safety evaluation of immune-based combinations in patients with advanced renal cell carcinoma: a systematic review and meta-analysis. *Expert Opin Drug Saf* 2020; 19: 1329–1338. DOI: 10.1080/14740338.2020.1811226.
- Rizzo A, Mollica V, Santoni M, et al. Impact of Clinicopathological Features on Survival in Patients Treated with First-line Immune Checkpoint Inhibitors Plus Tyrosine Kinase Inhibitors for Renal Cell Carcinoma: A Meta-analysis of Randomized Clinical Trials. *Eur Urol Focus* 2021; S2405-4569(21)00058-4. DOI: 10.1016/j.euf.2021.03.001.
- Lebacle C, Pooli A, Bessedé T, et al. Epidemiology, biology and treatment of sarcomatoid RCC: current state of the art. *World J Urol* 2019; 37: 115–123. DOI: 10.1007/s00345-018-2355-y.
- Parker WP, Chevillet JC, Frank I, et al. Application of the Stage, Size, Grade, and Necrosis (SSIGN) Score for Clear Cell Renal Cell Carcinoma in Contemporary Patients. *Eur Urol* 2017; 71: 665–673. DOI: 10.1016/j.eururo.2016.05.034.
- Tan HJ, Norton EC, Ye Z, et al. Long-term survival following partial vs radical nephrectomy among older patients with early-stage kidney cancer. *JAMA* 2012; 307: 1629–1635. DOI: 10.1001/jama.2012.475.
- Blum KA, Gupta S, Tickoo SK, et al. Sarcomatoid renal cell carcinoma: biology, natural history and management. *Nat Rev Urol* 2020; 17: 659–678. DOI: 10.1038/s41585-020-00382-9.
- Petitprez F, Ayadi M, de Reyniès A, et al. Review of Prognostic Expression Markers for Clear Cell Renal Cell Carcinoma. *Front Oncol* 2021; 11: 643065. DOI:10.3389/fonc.2021.643065.
- Na N, Si T, Huang Z, et al. High expression of HMGA2 predicts poor survival in patients with clear cell renal cell carcinoma. *Oncotargets Ther* 2016; 9: 7199–7205. DOI:10.2147/OTT.S116953.
- Kou B, Liu W, Tang X, Kou Q. HMGA2 facilitates epithelial-mesenchymal transition in renal cell carcinoma by regulating the TGF- $\beta$ /Smad2 signaling pathway. *Oncol Rep* 2018; 39: 101–108. DOI:10.3892/or.2017.6091.
- Vignali R and Marracci S. HMGA Genes and Proteins in Development and Evolution. *Int J Mol Sci* 2020; 21: 654. DOI:10.3390/ijms21020654.
- Shi X, Tian B, Ma W, et al. A novel anti-proliferative role of HMGA2 in induction of

- apoptosis through caspase 2 in primary human fibroblast cells. *Biosci Rep* 2015; 35: e00169. DOI: 10.1042/BSR20140112.
19. Wu Z, Wang M, Li F, et al. CDK13-Mediated Cell Cycle Disorder Promotes Tumorigenesis of High HMGA2 Expression Gastric Cancer. *Front Mol Biosci* 2021; 8: 707295. DOI:10.3389/fmolb.2021.707295.
  20. Dong J, Wang R, Ren G, et al. HMGA2-FOXJ2 Axis Regulates Metastases and Epithelial-to-Mesenchymal Transition of Chemo resistant Gastric Cancer. *Clin Cancer Res* 2017; 23: 3461–3473. DOI: 10.1158/1078-0432.CCR-16-2180.
  21. Di Fazio P, Mass M, Roth S, et al. Expression of hsa-let-7b-5p, hsa-let-7f-5p, and hsa-miR-222-3p and their putative targets HMGA2 and CDK in typical and atypical carcinoid tumors of the lung. *Tumor Biol* 2017; 39: 1010428317728417. DOI: 10.1177/1010428317728417.
  22. Sheldon LA. Inhibition of E2F1 activity and cell cycle progression by arsenic via retinoblastoma protein. *Cell Cycle* 2017; 16: 2058–2072. DOI: 10.1080/15384101.2017.1338221.
  23. Poppy Roworth A, Ghari F and La Thangue NB. To live or let die - complexity within the E2F1 pathway. *Mol Cell Oncol* 2015; 2: e970480. DOI: 10.4161/23723548.2014.970480.
  24. Xiao Q, Li L, Xie Y, et al. Transcription factor E2F1 is upregulated in human gastric cancer tissues and its overexpression suppresses gastric tumor cell proliferation. *Cell Oncol* 2007; 29: 335–349. DOI: 10.1155/2007/147615.
  25. Xing F, Song Z and He Y. MiR-219-5p inhibits growth and metastasis of ovarian cancer cells by targeting HMGA2. *Biol Res* 2018; 51: 50. DOI: 10.1186/s40659-018-0199-y.
  26. Cai J, Shen G, Liu S, et al. Downregulation of HMGA2 inhibits cellular proliferation and invasion, improves cellular apoptosis in prostate cancer. *Tumour Biol* 2016; 37: 699–707. DOI: 10.1007/s13277-015-3853-9.
  27. Zhang J, Zhang L, Xu Y, et al. Deciphering the binding behavior of flavonoids to the cyclin dependent kinase 6/cyclin D complex. *PLoS One* 2018; 13: e0196651. DOI: 10.1371/journal.pone.0196651.
  28. Kim CJ, Terado T, Tambe Y, et al. Anti-oncogenic activities of cyclin D1b siRNA on human bladder cancer cells via induction of apoptosis and suppression of cancer cell stemness and invasiveness. *Int J Oncol* 2018; 52: 231–240. DOI: 10.3892/ijo.2017.4194.
  29. Gundlach JP, Hauser C, Schlegel FM, et al. Prognostic significance of high mobility group A2 (HMGA2) in pancreatic ductal adenocarcinoma: malignant functions of cytoplasmic HMGA2 expression. *J Cancer Res Clin Oncol* 2021; 147: 3313–3324. DOI:10.1007/s00432-021-03745-w.
  30. Liu Y, Fu QZ, Pu L, et al. Effect of RNA interference of the expression of HMGA2 on the proliferation and invasion ability of ACHN renal cell carcinoma cells. *Mol Med Rep* 2017; 16: 5107–5112. DOI:10.3892/mmr.2017.7258.
  31. Jian Y, Yang K, Sun X, et al. Current Advance of Immune Evasion Mechanisms and Emerging Immunotherapies in Renal Cell Carcinoma. *Front Immunol* 2021; 12: 639636. DOI:10.3389/fimmu.2021.639636.
  32. Angulo JC, Manini C, López JI, Pueyo A, Colás B, Ropero S. The Role of Epigenetics in the Progression of Clear Cell Renal Cell Carcinoma and the Basis for Future Epigenetic Treatments. *Cancers (Basel)* 2021; 13: 2071. DOI:10.3390/cancers13092071.
  33. Zhao XP, Zhang H, Jiao JY, et al. Overexpression of HMGA2 promotes tongue cancer metastasis through EMT pathway. *J Transl Med* 2016; 14: 26. DOI: 10.1186/s12967-016-0777-0.
  34. Wei L, Liu X, Zhang W, et al. Overexpression and oncogenic function of HMGA2 in endometrial serous carcinogenesis. *Am J Cancer Res* 2016; 6: 249–259.
  35. Li X, Wang S, Li Z, et al. The lncRNA NEAT1 facilitates cell growth and invasion via the miR-211/HMGA2 axis in breast cancer. *Int J Biol Macromol* 2017; 105: 346–353. DOI: 10.1016/j.ijbiomac.2017.07.053.
  36. Singh I, Mehta A, Contreras A, et al. Hmga2 is required for canonical WNT signaling during lung development. *BMC Biol* 2014; 12: 21. DOI:10.1186/1741-7007-12-21.
  37. Su L, Deng Z and Leng F. The Mammalian High Mobility Group Protein AT-Hook 2 (HMGA2): Biochemical and Biophysical

- Properties, and Its Association with Adipogenesis. *Int J Mol Sci* 2020; 21: 3710. DOI:10.3390/ijms21103710.
38. Sun X, Xu M, Liu H, et al. MicroRNA-219 is downregulated in non-small cell lung cancer and inhibits cell growth and metastasis by targeting HMGA2. *Mol Med Rep* 2017; 16: 3557–3564. DOI: 10.3892/mmr.2017.7000.
39. Kaur H, Ali SZ, Huey L, et al. The transcriptional modulator HMGA2 promotes stemness and tumorigenicity in glioblastoma. *Cancer Lett* 2016; 377: 55–64. DOI: 10.1016/j.canlet.2016.04.020.
40. Banjara S, Suraweera CD, Hinds MG, et al. The Bcl-2 Family: Ancient Origins, Conserved Structures, and Divergent Mechanisms. *Biomolecules* 2020; 10: 128. DOI:10.3390/biom10010128.
41. Singh R, Letai A and Sarosiek K. Regulation of apoptosis in health and disease: the balancing act of BCL-2 family proteins. *Nat Rev Mol Cell Biol* 2019; 20: 175–193. DOI:10.1038/s41580-018-0089-8.
42. Boice A and Bouchier-Hayes L. Targeting apoptotic caspases in cancer. *Biochim Biophys Acta Mol Cell Res* 2020; 1867: 118688. DOI:10.1016/j.bbamcr.2020.118688.
43. Vogeler S, Carboni S, Li X, et al. Phylogenetic analysis of the caspase family in bivalves: implications for programmed cell death, immune response and development. *BMC Genomics* 2021; 22: 80. DOI:10.1186/s12864-021-07380-0.
44. Panneer Selvam S, Roth BM, Nganga R, et al. Balance between senescence and apoptosis is regulated by telomere damage-induced association between p16 and caspase-3. *J Biol Chem* 2018; 293: 9784–9800. DOI:10.1074/jbc.RA118.003506.
45. Li P, Zhou L, Zhao T, et al. Caspase-9: structure, mechanisms and clinical application. *Oncotarget* 2017; 8: 23996–24008. DOI:10.18632/oncotarget.15098.
46. Rahman MA, Shirai M, Aziz MA, et al. An epistatic effect of apaf-1 and caspase-9 on chlamydial infection. *Apoptosis* 2015; 20: 1271–1280. DOI:10.1007/s10495-015-1161-x.
47. Amiri S, Rabbani-Chadegani A, Davoodi J, et al. Restoration of MiR-34a Expression by 5-Azacytidine Augments Alimta-Induced Cell Death in Non-Small Lung Cancer Cells by Downregulation of HMGB1, A2 and Bcl-2 Pathway. *Cell J* 2021; 23: 674–683. DOI:10.22074/cellj.2021.7332.
48. Block KI, Gyllenhaal C, Lowe L, et al. Designing a broad-spectrum integrative approach for cancer prevention and treatment. *Semin Cancer Biol* 2015; 35 (Suppl): S276–S304. DOI:10.1016/j.semcancer.2015.09.007.
49. Yang Q, Ren GL, Wei B, et al. Conditional knockout of TGF- $\beta$ RII/Smad2 signals protects against acute renal injury by alleviating cell necroptosis, apoptosis and inflammation. *Theranostics* 2019; 9: 8277–8293. DOI: 10.7150/thno.35686.
50. Aragón E, Wang Q, Zou Y, et al. Structural basis for distinct roles of SMAD2 and SMAD3 in FOXH1 pioneer-directed TGF- $\beta$  signaling. *Genes Dev* 2019; 33: 1506–1524. DOI: 10.1101/gad.330837.119.
51. Kaszak I, Witkowska-Piłaszewicz O, Niewiadomska Z, et al. Role of Cadherins in Cancer-A Review. *Int J Mol Sci* 2020; 21: 7624. DOI: 10.3390/ijms21207624.
52. Wang W, Hu W, Wang Y, et al. Long non-coding RNAUCA1 promotes malignant phenotypes of renal cancer cells by modulating the miR-182-5p/DLL4 axis as a ceRNA. *Mol Cancer* 2020; 19: 18. DOI: 10.1186/s12943-020-1132-x.
53. Yang L, Zou X, Zou J, et al. A Review of Recent Research on the Role of MicroRNAs in Renal Cancer. *Med Sci Monit* 2021; 27: e930639. DOI: 10.12659/MSM.930639.
54. Balan M, Chakraborty S, Flynn E, et al. Honokiol inhibits c-Met-HO-1 tumor-promoting pathway and its cross-talk with calcineurin inhibitor-mediated renal cancer growth. *Sci Rep* 2017; 7: 5900. DOI: 10.1038/s41598-017-05455-1.